

On the impact of the physical layer model on the performance of D2D-offloading in vehicular environments

Loreto Pescosolido, Marco Conti, Andrea Passarella

Italian National Research Council,

Institute for Informatics and Telematics (CNR-IIT), Pisa, Italy

Abstract

Offloading data traffic from Infrastructure-to-Device (I2D) to Device-to-Device (D2D) communications is a powerful tool for reducing congestion, energy consumption, and spectrum usage of mobile cellular networks. Prior network-level studies on D2D data offloading focus on high level performance metrics as the *offloading efficiency*, and take into account the radio propagation aspects by using simplistic wireless channel models. In this work, we consider a D2D data offloading protocol tailored to highly dynamic scenarios as vehicular environments, and evaluate its performance focusing on physical layer aspects, like *energy consumption and spectral efficiency*. In doing this, we take into account more realistic models of the wireless channel, with respect to the simplistic ones generally used in the previous studies. Our objective is twofold: first, to quantify the performance gain of the considered D2D offloading protocol with respect to a classic cellular network, based on I2D communications, in terms of energy consumption and spectral efficiency. Second, to show that using simplistic channel models may prevent to accurately evaluate the performance gain. Additionally, the use of more elaborated models allows to obtain insightful information on relevant system-level parameters settings, which would not be possible to obtain by using simple models. The considered channel models range from widely used models based on deterministic path loss formulas, to more accurate ones, which include effects like multipath fading and the associated frequency selectivity of wideband channels. These models have been proposed and validated, in the recent years, through large-scale measurements campaigns.

Our results show that the considered protocol is able to achieve a reduction in the energy consumption of up to 35%, and an increase in the system spectral efficiency of 50%, with respect to the benchmark cellular system. The use of different channel models in evaluating these metrics may result, in the worst case, in a sixfold underestimation of the achieved improvement.

Keywords: D2D data offloading, caching, vehicular networks

1. Introduction

Offloading the delivery of contents to mobile users from traditional Infrastructure to Device (I2D) to Device-to-Device (D2D) communication, [1], is beneficial from many standpoints:

i) Traffic congestion at the Base Station (BSs) can be reduced, since it is no more necessary that a BS transmits the same content to different devices that have requested it at close-by instants and are close to each other.

ii) Thanks to their smaller transmission range, D2D communications require less transmit power than I2D ones, entailing a reduction of the overall energy consumption at the system level. *iii)* Thanks to the increased spa-

Email address: loreto.pescosolido@iit.cnr.it, marco.conti@iit.cnr.it, andrea.passarella@iit.cnr.it (Loreto Pescosolido, Marco Conti, Andrea Passarella)

tial frequency reuse made possible by the small footprint of D2D communications, with respect to I2D ones, it is possible to increase the overall system spectral efficiency, defined as the ratio between the amount of delivered bits and the amount of radio resources in use, e.g., the Physical Resource Blocks (PRBs) of a LTE-A time-frequency grid.

The presence of multipath fading and, in the case of wideband systems, frequency selectivity, has a notable importance in the determination of the transmit power used by the devices. Furthermore, by allowing concurrent links to reuse the same radio resources, interference among links becomes one of the major factors limiting the system performance, and interference is highly dependent on fading and frequency selectivity. Therefore, a careful performance evaluation of D2D data offloading protocols, focusing on physical quantities like energy consumption and spectrum usage, requires an accurate modeling of the radio propagation aspects. However, most network-level studies on D2D offloading schemes, as well as many radio resource allocation schemes for concurrent D2D communications, assume relatively simplistic channel models. While using these models is instrumental to simplify the analysis and devise effective offloading algorithms, we argue that an accurate performance evaluation should take into account more realistic channel models.

In this work, we build upon the offloading scheme presented in [2] and devise a Content Delivery Management System (CDMS), operated by the network infrastructure in a distributed way. The CDMS implements an offloading strategy suitable for dynamic scenarios like vehicular networks. We evaluate the performance of the resulting protocol in terms of energy consumption and spectral efficiency, by considering realistic *frequency selective* channel models. Our work extends the analysis of the protocol presented in [2] by considering multiple contents of interest, with different popularity. The considered protocol falls within

the class of D2D data offloading protocols (see e.g., [3, 4, 5, 6], and [1] for an extensive survey). Most of the works in this area focus on high level networking aspects and performance metrics, while an evaluation of metrics more related to physical quantities of interest like energy consumption and spectrum occupation, based on accurate wireless channel models, is missing.

The channel models considered in this work have been developed in the last years in the context of large European projects [7, 8] by exploiting measurement campaigns conducted by major telecom companies like Nokia and Docomo, and have been received by standardization bodies [9, 10]. To make our evaluation realistic, we introduced in our system model an LTE-like MAC layer, with radio resources organized in a time-frequency grid, and devised a scheduling procedure, inspired by [11], for allocating the radio resources to the I2D communications and D2D communications.

Regarding the performance gain of our offloading protocol, with respect to a system using exclusively I2D communications, we found, for the considered system parameters, an increase in both energy efficiency and spectral efficiency around 50%. Furthermore, considering the inaccuracy in the estimation of the entity of the performance gain using simplistic models, there can be deviations of up to one fifth (20%), e.g., over an estimated value of a 32% spectrum usage reduction (obtained using the most accurate wireless channel model). Preliminary results of this study have been presented in [12], although under simplified assumptions for the transmission, interference, and packet error model¹, whereas in [13] we have devised an analytical model to compute the offloading efficiency and energy consumption of the CDMS considered in this work.

¹In [12], we assumed an ideal resource allocation, without considering interference among concurrent D2D or I2D links, and focused on energy consumption only.

The paper is organized as follows: in Section 2 we provide the details of the considered channel models. Section 3 presents our CDMS. Section 4 describes a radio resource allocation scheme on top of which the CDMS can be implemented, and a physical layer model suitable to capture the effect of frequency selectivity on wideband communications, while keeping the complexity of the implementation in a system level simulator to an acceptable level. In Section 5 we evaluate the performance of the proposed offloading system, highlighting how the wireless channel model affects the performance evaluation. Finally, in Section 6, we conclude the paper, summarizing our contributions and findings.

2. Channel modeling approach

Many existing works on D2D-based traffic offloading involve a system-level performance evaluation where simple channel models are used to establish the peer-to-peer connectivity between neighboring devices, and the interference among simultaneous transmissions on the same radio channels. Popular models are, for instance, the “protocol interference” model [14], channel models with deterministic path losses, or flat fading channels with Rayleigh fading. These models, thanks to their simplicity, allow to evaluate high level performance metrics in large scale networks in a relatively accurate way, but fall short when considering metrics more directly related to physical quantities. One high level metric, for instance, is offloading efficiency, defined as the percentage of contents delivered through D2D communications, [1], [2]. However, while this metric captures in a single parameter the effectiveness of the considered offloading protocol in achieving its objective, a more in-depth performance evaluation, which can be more easily mapped to the cost incurred by the network operators and the users, needs to target metrics like energy consumption and spectral efficiency. Therefore, the performance evaluation, in this work, focuses on the latter two metrics.

When considering performance metrics such as energy consumption and spectral efficiency, simplistic channel models are not sufficiently accurate. In real-life deployments, shadowing, multipath small scale fading, Line Of Sight (LOS) or Non Line Of Sight (NLOS) conditions, induce large variations of both the useful signal and the interfering signals strengths. For a given transmitter-receiver distance, such variations can be in the range of tens of dBs. Furthermore, the Large Scale Parameters (LSPs) of the random components of the channel attenuation² exhibit spatial correlation³, and correlation among different parameters for the same link. Additionally, they are also scenario-dependent⁴ [7, 8, 9, 10], and in the same scenario they depend on the communication being either D2D or I2D. Finally, in existing wideband systems, frequency selectivity due to multipath fading is also an important physical layer aspect that needs to be taken into account for an accurate performance evaluation.

In this work, motivated by the multitude of physical effects overlooked by widely used simplistic models, we adopt the geometry-based stochastic channel model (GSCM) put forward by the WINNER II European project in [7] and subsequently refined/extended by the ITU [9], the 3GPP [10], and by the METIS Project [8]. Specifically, in [9], a detailed procedure is described for generating a set of frequency selective channels affected by shadowing and small scale fading. The procedure uses specific, scenario-dependent, formulas (that are

²LSPs include, but are not limited to, first and second order moments of LogNormal shadowing, Rician K-Factor (used to parameterize the small scale fading probability distribution), and channel impulse response delay spread.

³Spatial correlation means that the LSPs of two different links with a common transmitter (or receiver) are correlated, and the correlation coefficient depends on the distance between the two receivers (or transmitters).

⁴The term “scenario”, here, refers to the characteristics of the real-life deployment environment, such as urban macro cell, urban micro cell, rural, etc..

provided by the above referenced reports), for computing the path loss and generating the set of LSPs.

In order to develop a large scale network level simulator, able to cope with tens or hundreds of nodes, we implemented the detailed channel models developed by the WINNER II and METIS Projects [7, 8, 9, 10], although skipping some details, like the intra-path superimposition of micro-paths, which would increase the complexity and memory usage of the simulator to an unnecessary (for our purposes) level. Our implementation is based on a discretized 2D representation of the Region Of Interest (ROI). It first involves the computation of the path loss between any two points in a 2D rectangular grid with a spatial step of 5 m in both dimensions, and between each Base Station (BS) and each point in the grid. To do this, we used the scenario-dependent formulas recommended in [8] for the Urban micro-cell (UMi) and Urban macro-cell (UMa) scenarios. Then, random correlated LSPs are generated for each link. Finally, the set of multipath channels, including random amplitude and delay for each signal replica that arrives at the receiver (through the multiple paths), is generated. This is done according to the procedure described in [7] for the GSCM model. While the procedure we used is the one presented in [7], we parameterized all the formulas to generate the LSPs and the impulse responses with the updated parameter values proposed in [8], for the UMi and UMa scenarios, and for both I2D and D2D communications⁵. In this work, we assume omnidirectional antennas and account for the different heights of the transmitting antenna for I2D and D2D communications (which do have an effect on the path loss values). Specifically, we consider an antenna height of 10 m and 25 m for

⁵Notably, [8] also includes parameter sets specific of D2D communications (which differ from I2D ones in that transmitter and receiver, in the D2D case, are typically at the same height, which is not the case for I2D communications).

BSs (for the UMi and UMa case, respectively) and 1.5 m for mobile devices, as recommended in [8, 9]. The models in [7, 9, 10, 8] provide a further level of detail, which we decided to skip as they are not relevant to our scenario and would unnecessarily increase the complexity of the simulator⁶.

3. D2D data offloading scheme with delayed content delivery

In D2D Data offloading schemes, D2D communications occur as mobile devices, although they can obtain a desired content by the infrastructure, i.e., the BSs, would preferably receive it from neighboring devices, that have cached the content previously. Offloading protocols require that a mobile device, upon receiving a content, keeps it cached, for some time, in order to share it with neighbors which will request it within the amount of time it is kept in the cache.

In static or quasi-static scenarios, a content request from a device is typically fulfilled immediately: either at the time of request there is a device (close-by the requesting device) with the content in its cache, which shares it with the requesting device, or, if there is no such neighboring device, the requesting device receives the content from a BS. However, in highly dynamic scenarios, such as in vehicular environments, thanks to the nodes' mobility, even though a certain content may be unavailable from the neighbors of the requesting device at the request time, it could still be obtained through a D2D link, later on, from a *new* neighboring device, which has previously cached the content. The new neighboring device is just a device that has come close to the requesting device *after* the content request time. To exploit this possibility, the offloading strategy presented in [2], uses a *content timeout*, i.e., an interval starting at the content request instant, during which

⁶Most of the details we skipped become relevant when dealing with directional antennas, multi-element antennas, and MIMO communications, which we do not consider in this work.

the requesting node tries to obtain the content from the devices it encounters. If this is not the case, the content is delivered to the node by a BS, at the expiration of the content timeout. In this way, the system offloading efficiency can be increased, with respect to the choice of transmitting the content immediately, either by a neighbor (if available) or by a BS. Typically, this approach can be taken for contents related to non delay-critical applications for which it is reasonable to accept that the content, instead of being retrieved immediately, can be obtained in a matter of seconds, or tens of seconds, depending on the application. Moreover, this approach works also when content requests are not synchronised, and therefore the BS cannot serve multiple mobile nodes through multicast transmissions.

In this work, we propose a CDMS that controls this type of offloading system. The CDMS is implemented as a distributed software agent that can communicate and track the users along their paths through the ROI. The proposed CDMS executes a protocol that implements the same offloading strategy of [2]. However, whereas in [2] the implementation of the offloading strategy is distributed at the device level, our CDMS mostly relies on control operations executed, still in a distributed way, at the network infrastructure nodes. Hence, whereas [2] largely relies on the self-organization capabilities of the devices, our protocol implements an infrastructure-assisted D2D communication approach. The motivation is that, in highly dynamic scenarios, the signaling required by the neighbor discovery protocol and content requests notifications of completely decentralized solutions may be excessive, if performed exclusively by the nodes, given that the network topology is continuously changing and its representation needs to be kept up to date.

3.1. Content delivery management

We consider a ROI populated with mobile users (humans, vehicles) each carrying a wireless device. Specifically, we assume that mobile

devices are on board of vehicles. The devices may be either human hand-held devices whose owners are in the vehicles, or wireless devices installed in the vehicle equipment. Users enter, roam into, and exit the ROI. As a vehicle enters the ROI, its on board device starts requesting contents according to a given content request process⁷. The content request process is characterized by a content-request *arrival* process, which defines the time instants at which the requests are generated, and a content-interest probability distribution, which defines which content is requested. We assume that the requests instants of different devices are statistically independent, and that the specific contents requested by different devices, or by the same device in different requests, are also independent. In Section 5, we provide the specific models for the nodes' mobility and the content request process used in our simulations. However, our protocol does not require the knowledge of these models.

During its path within the ROI, at each instant, each device is associated to a BS, which is responsible of handling the delivery of the contents requested by that device. For each device k associated to a BS, the BS holds a list of neighbors \mathcal{N}_k composed of pairs of the form (j, r_j^k) , where j is the id of any node which is a neighbor of node k , and r_j^k is a ranking index of node j as "seen" by node k on the basis of a given criterion. In this work, the criterion to establish if two nodes are neighbors, and the ranking of each node's neighbors, is based on a nominal indicator of the channel quality between the nodes. In general, the nominal channel quality may be computed, by the CDMS, on the basis of the positions of the nodes, which the BSs are assumed to know, using a given channel model. In the following, we indicate this measure as *nominal channel gain*. Assum-

⁷The content request process is originated at the application layer. Here, it is of no importance whether the interest is generated by a human or by, for instance, an IoT application executed by the software on a vehicle.

ing a deterministic model for the computation of the *nominal* channel gain (i.e., that the nominal channel gain g is a monotonically decreasing function of the distance d), two nodes are considered as neighbors, by the CDMS, in the time instants their distance is less than or equal to a maximum value d_{\max} . In this work, we assume that a deterministic model is used to determine if two nodes are neighbors⁸.

The CDMS, essentially, acts on a distributed database containing the up to date list of each node's position, the list of its neighbors, and the nominal channel gain between any two neighbors and between each node and the surrounding BSs. The CDMS can be implemented as a distributed software agent, for instance, through a Network Function Virtualization (NFV) component allocated appropriately in the infrastructure topology. The BSs are used by the CDMS to operate the offloading protocol. To handle the handover of ongoing requests originated from a node that crosses a cell border while waiting for a content, adjacent BSs periodically exchange the up to date status of the ongoing request procedures (see below) of the nodes moving across cells⁹. At each BS, the lists \mathcal{N}_k are updated on the basis of Hello messages, sent periodically by the nodes, containing their id. Each node k has an internal content cache \mathcal{C}_k populated with previously downloaded contents. At any time, the CDMS also has an index of the contents in each node's cache, although the CDMS does not necessarily hold a copy of the contents.

Based on this available information, following a content request by device k for content

⁸More sophisticated techniques may be considered to determine the nominal channel gain. For instance, it may be computed taking into account slowly varying shadowing statistics between any two points in the (discretized) space. This would require means to create such a shadowing map. This is an interesting research issue which we will consider in future works.

⁹This information exchange can be performed using high speed fiber connections, or dedicated radio channels forming a wireless mesh-type backhaul component of the Radio Access Network (RAN).

z , the CDMS determines the content delivery time and mode. Three cases are possible:

1) At the request time, node k has at least one neighbor with the content z available. In this case, the CDMS prompts the closest neighbor with content z available to transmit it to node k .

2) At the request time, node k has no neighbors with the content z available, but during the content timeout, as a consequence of the mobility of the devices, a device with the content available comes within the range d_{\max} of the node k . In this case, as soon the CDMS detects that such condition is verified, it prompts the node that has come within the range d_{\max} to immediately transmit the content to node k .

3) No neighbor of node k , either at the request time, or during the content timeout, has content z in cache. In this case, at the end of the content timeout, the CDMS prompts the transmission of content z by the infrastructure, i.e., by the closest BS.

The pseudocode in Algorithms 1 and 2 describes in more detail the actions taken on demand, i.e., as a consequence of content requests, by the nodes and the CDMS. We briefly introduce the notation required for a correct interpretation of the algorithms: the notation $\biguplus \{\mathcal{C}_j | \text{condition on } j\}$ is used to indicate the union of the caches of nodes satisfying a given condition; the notation $\hat{j}(k, z)$ is used to indicate the node j that has the best ranking r_j^k among the neighbors of node k which have content z in their caches; the notation $j \xrightarrow{z} k$ indicates the transmission of content z from node j to node k . These transmissions are triggered by the CDMS. The remaining notation used in Algorithms 1-2 is self-explaining.

Algorithm 1 describes the actions of a node as it becomes interested in a content. Essentially, it notifies the CDMS that it is interested in that content, and then waits for receiving it either from a BS or from a neighbor. The system guarantees that the content will be delivered within a given *content timeout*. After the reception of the content, the node makes

Algorithm 1 Actions taken by node k to request content z

```

1: Upon request for content  $z$  from the application layer
2: Set  $k\_content\_received = \text{false}$ 
3: Send  $(k, z)\_cont\_req$  to CDMS
4: while  $k\_content\_received == \text{false}$  do
  ▷ Wait for receiving content  $z$ , from a BS or from a neighbor
5:   if content  $z$  is received then
6:     Set  $k\_content\_received = \text{true}$ 
7:     Send  $(k, z)\_ACK$  to CDMS and/or the sending node
8:     Add  $z$  to  $\mathcal{C}_k$ 
9:     Set  $(k, z)\_sharing\_timeout$ 
10:    break
11:   end if
12: end while
13: while  $(k, z)\_sharing\_timeout$  is not expired do
  ▷ Available for opportunistic sharing of content  $z$ 
14:   Upon request from CDMS (step 7 of Algorithm 2)
15:   Send  $z$  to node requesting it
16: end while
17: Remove content  $z$  from  $\mathcal{C}_k$ 
18: Cancel  $(k, z)\_sharing\_timeout$ 

```

it available for other nodes that may request it, for a limited amount of time determined by a *sharing timeout*. The sharing timeout is required to avoid cache overflow.

Algorithm 2 describes the actions taken by the CDMS to handle a content request. Here, a key point, which allows to further reduce the system energy consumption, is that the CDMS selects the best node for delivering the content, on the basis of channel quality considerations, represented by the ranking of each node's neighbors (steps 5-13). If, however the content cannot be delivered through a D2D communication within the content timeout, the CDMS uses the BSs to deliver it (steps 15-20).

Algorithm 2 Actions taken by CDMS for handling content request (k, z)

```

1: Upon receiving  $(k, z)\_cont\_req$ 
2: Set  $(k, z)\_served = \text{false}$ 
3: Set  $(k, z)\_content\_timeout$ 
4: while  $(k, z)\_content\_timeout$  is not expired do
5:   if  $z \in \bigcup \{\mathcal{C}_j | j \in \mathcal{N}_k\}$  then
6:     Identify  $\hat{j}(k, z)$ 
7:     Trigger transmission  $\hat{j}(k, z) \xrightarrow{z} k$ 
8:     Wait for  $(k, z)\_ACK$ 
9:     Upon  $(k, z)\_ACK$  reception
10:    Set  $(k, z)\_served = \text{true}$ 
11:    Remove  $(k, z)$  from  $\mathcal{L}_{req}$ 
12:    break
13:   end if
14: end while
15: if  $(k, z)\_served == \text{false}$ 
16:   Send  $z$  to  $k$ 
17:   Wait for  $ACK\_ (k, z)$ 
18:   Upon reception of  $ACK\_ (k, z)$ 
19:   Set  $(k, z)\_served = \text{true}$ 
20: end if
21: Cancel  $(k, z)\_content\_timeout$ 

```

4. Radio resource allocation, transmission, and error model

4.1. In-band radio resource reuse

To evaluate the energy consumption and the spectral efficiency of our protocol, we implemented a MAC layer structure exploiting the time-frequency domain, and designed a scheduling and resource allocation protocol that handles the transmission of contents through either D2D or I2D communications. The BSs schedule both the transmission of I2D and D2D packets with the periodicity of a control interval (CI) of duration T_{CI} , using an overall system bandwidth W . In each CI, the radio resources are organized in a grid over a time-frequency frame of duration T_{CI} and bandwidth W . Each grid element is a Physical Resource Block (PRB) of duration τ and bandwidth w . We indicate the number of PRBs in a CI as N_{PRB} . The bandwidth of a PRB contains n_c

subcarriers, each of bandwidth (or subcarrier spacing) $w_c = w/n_c$. For each CI, a fine grain scheduling procedure has to be executed, which determines which PRBs will be used by all the involved nodes to transmit the packets that the CDMS has selected for transmission in that CI. To distinguish it from the scheduling performed by the CDMS, which acts on a coarser time scale, in the order of the content timeout duration, we call Radio Resource (RR) scheduler the scheduler that, in each CI, effectively allocates PRBs to each link (and for each link, to the packets that have to be transmitted over it). The RR scheduler is not the focus of this work, but serves as a baseline implementation to analyze the performance of our CDMS in a realistic setting. Therefore, for the sake of readability, we provide here a high level description, while a more detailed description is presented in the Appendix.

To leverage spatial frequency reuse, we have devised a RR scheduler inspired by the “full resource sharing” approach of [11]. With this approach, multiple concurrent D2D communications can share the same PRBs, and each PRB can be assigned also to, at most, a single I2D link within a cell and across adjacent cells. The considered approach is particularly attractive since it allows to exploit spatial frequency reuse to its extreme, outperforming other conventional approaches like user-oriented resource sharing or resource-oriented resource sharing [11]. For the purpose of this work, however, the RR scheduler proposed in [11] cannot be directly applied, since it is devised under the assumptions of a single cell, uniform transmit power for all D2D communications and for all I2D communications, and flat fading channels. Additionally, in [11], resources are allocated to links with the granularity of a single radio resource (for us, a PRB), with the objective to maximize throughput. With our setup, in which there is a predefined content to be transmitted by each scheduled link in each CI, this could result in a link receiving an amount of ra-

dio resources which is not sufficient to transmit the desired content within a CI¹⁰. Therefore, our radio resource allocation, although inspired by the one presented in [11], differs from it in several aspects. Our implementation of the RR scheduler includes an admission control which limits the number of both I2D and D2D packets that can be transmitted using the resources in a CI, based on an iterative validation of cross-link interference constraints (see the Appendix). If a packet transmission cannot fit, it is pruned, and postponed to the next CI. These episodes may occur, for instance, during localized traffic load peaks. Note that, in general, the latencies introduced due to pruning, and to transmission errors (with the associated retransmissions) are negligible with respect to the order of magnitude of the delay-tolerance (tens of seconds), i.e., the content-timeout¹¹. Delays due to transmissions errors and pruning, however, are actually reproduced in our simulations.

In the following, we indicate with S the set of radio links that are scheduled for transmission in a given CI. A link i represents a transmitter-receiver pair (x_i, y_i) . In our setup, x_i can be either a BS or a mobile device, whereas y_i is always a mobile device. Let k be the generic PRB in a CI, $k \in \{1, \dots, N_{\text{PRB}}\}$, and p an index over the packets that are scheduled to be transmitted during the CI. The output of the RR scheduler can be represented by the set of indicator functions $\phi_{i,k}(p)$, $\forall i \in S, \forall k \in \{1, \dots, N_{\text{PRB}}\}$, which tells that link i uses PRB k to transmit packet p , i.e.,

$$\phi_{i,k}(p) = \begin{cases} 1 & \text{if PRB } k \text{ is used by link } i \\ & \text{to transmit content } p \\ 0 & \text{otherwise} \end{cases} . \quad (1)$$

¹⁰For simplicity, our MAC does not consider packet fragmentation over multiple CIs.

¹¹Note that the content timeout parameter may also be set in a conservative way, e.g., 1 or 2 seconds less than the actual delay tolerance.

4.2. Physical layer and transmission error model

In the following, we describe a physical layer model which enables to perform large scale network-level simulations while retaining (to an acceptable extent) the representation of the effect of important physical layer parameters that are tightly related to the wireless channel model: shadowing, fading, and frequency selectivity.

We assume a multicarrier modulation with a uniform power allocation over all the subcarriers in use. We denote with $P_i^{(c)}$ the transmit power used by the transmitter of link i on each subcarrier it uses, and with $H_{\langle j,i \rangle}(f)$ the channel transfer function of the radio channel between the transmitter of link j and the receiver of link i . Considering the PRB k , we enumerate its n_c subcarriers as $f_1^{(k)}, \dots, f_{n_c}^{(k)}$. The Signal to Noise Plus Interference Ratio (SNIR) for link i in the q -th subcarrier of PRB k is

$$\xi_{i,q}^{(k)} = \frac{P_i^{(c)} \left| H_{\langle i,i \rangle} \left(f_q^{(k)} \right) \right|^2}{\sigma_c^2 + \sum_{j \in S \setminus \{i\}} \psi_{j,k} P_j^{(c)} \left| H_{\langle j,i \rangle} \left(f_q^{(k)} \right) \right|^2}, \quad (2)$$

where σ_c^2 is the noise power on each subcarrier. Specifically, $\sigma_c^2 = w_c F N_0$, where N_0 is the thermal noise power spectral density, and F is the noise figure of the receiver.

Our error model for the transmission, on link i , of a content p of size $L(p)$ payload bits, using the PRBs allocated to its transmission by the RR scheduler, consists in verifying that the corresponding *achievable amount of information*¹² transferrable by link i in those PRBs is larger than or equal to $L(p)$.

¹²We use the term ‘‘achievable amount of information’’ of a transmission over a subcarrier, in an information theoretic sense. Specifically, we define it as the product of a Shannon capacity, haircut by a maximum transmit spectral efficiency (i.e. a given maximum number of bits that can be loaded on each symbol of the digital modulation scheme in use), times the duration of the transmission.

The Shannon capacity of a single subcarrier, normalized to its bandwidth, is given by $\log_2(1 + \xi_{i,q}^{(k)})$, where $\xi_{i,q}^{(k)}$ is given by (2). Let e_i be the *transmit spectral efficiency* (i.e., the maximum number of bits that can be carried by a single symbol of the digital modulation scheme in use, over a subcarrier) of link i , measured in bits per second per Hertz (bps/Hz). In real systems, a subcarrier use cannot carry an amount of information larger than e_i , even when its Shannon capacity is larger than it. Therefore, we compute the contribution of, say, the q -th subcarrier used in a given PRB k (i.e., for the duration of a time slot), to the achievable amount of information, as $\tau w_c \min(e_i, \log_2(1 + \xi_{i,q}^{(k)}))$. Summing up all the contributions of this kind, on the basis of the PRBs allocated to the transmission of a packet p (indicated by the function $\phi_{i,k}^{(p)}$ by the RR scheduler, and imposing that the sum is larger than the amount of *payload* bits, we obtain the following inequality, with which we model a packet transmission success:

$$\tau w_c \sum_{k=1}^{N_{\text{PRB}}} \phi_{i,k}^{(p)} \sum_{q=1}^{n_c} \min(e_i, \log_2(1 + \xi_{i,q}^{(k)})) \geq L(p). \quad (3)$$

If (3) is satisfied, the packet is successfully received, otherwise, we count a failed transmission.

Up to now, we have left unspecified the settings of two important parameters: the transmit power $P_i^{(c)}$ appearing in Eq. (2), and the number of PRBs to be allocated to a packet transmission, i.e, the number of nonzero terms in the double sum of the left hand side of (3). The latter parameter is determined by the need to encode each content in a packet that has a size, $D(p)$, which is, in general, larger than $L(p)$. We discuss these two parameters in the following subsection.

4.3. Physical layer parameters: link margin and forward error correction

In the practical deployment of any wireless network which uses power control based on nominal channel gains, the transmitter needs to compensate for the presence of random shadowing and multipath fading. In our case, these random effects are not factored in by the nominal channel gain $g_{\langle i,i \rangle}$ (on which $P_i^{(c)}$ depends). Moreover, in the presence of concurrent links using the same radio resources, the effect of the interference coming from the links using the same PRBs must also be taken into account. The typical tools to deal with these problems, are: i) a transmit power link margin, added on top of the power that would be required for transmitting over an ideal deterministic channel with flat frequency response, ii) Forward Error Correction (FEC), or, more in general, Adaptive Modulation and Coding (AMC) (see below).

We model the use of FEC as follows: we consider a coding rate parameter, which we indicate as K_{ec} , defined as the ratio between the payload size L and the coded packet size D , or $K_{ec} = L/D$. K_{ec} is a characteristic figure of the FEC code in use, which tells how much redundancy is introduced in the coded packets to increase the resiliency to noise and interference. The lower K_c , the higher the redundancy, at the price of a larger number of bits to be transmitted, for a given payload. The selected coding rate (and hence number of *coded* bits D), in our model, determines the number of nonzero elements in the right hand side of (3), i.e., those for which $\phi_{i,k}^{(p)} = 1$). The *specific* elements for which $\phi_{i,k}^{(p)} = 1$ are the output of the RR scheduler.

Considering an AMC system, the power allocated over a subcarrier (excluding the power margin) would be set to the power required to support a target normalized information rate equal to a transmit spectral efficiency selected within a discrete set $\{e_{\min}, \dots, e_{\max}\}$, representing, e.g., the use of different digital symbols

constellations.

We set the power $P_i^{(c)}$ appearing in Eq. (2) as

$$P_i^{(c)} = M \frac{\sigma_c^2}{g_{\langle i,i \rangle}} (2^{\bar{e}_i} - 1), \quad (4)$$

where $g_{\langle i,i \rangle}$ is the nominal channel gain of link i , \bar{e}_i is a target normalized information rate (measured in bps/Hz) that the communication aims to achieve, and M is a suitable link margin. The term $\frac{\sigma_c^2}{g_{\langle i,i \rangle}} (2^{\bar{e}_i} - 1)$ is the transmit power per subcarrier that would be required to support the desired normalized information rate, \bar{e}_i , over an ideal link with a flat fading channel whose gain is $g_{\langle i,i \rangle}$. In dBm, the per-subcarrier transmit power is given by

$$P_{i,[dBm]}^{(c)} = \sigma_{c,[dBm]}^2 - g_{\langle i,i \rangle}[dB] + 10 \log_{10} (2^{\bar{e}_i} - 1) + M_{[dB]}. \quad (5)$$

The above described physical layer model is able to reproduce the behavior of (coexisting) communications occurring on wideband frequency selective channels, taking into account the power link margin and AMC parameters like FEC coding rate and constellation size, without the need to simulate the transmission at the symbol level (which would make it quite hard to perform system level simulations involving hundreds of nodes). Furthermore, the RR scheduler we devised based on [11], can exploit different settings of the said parameters (link margin, FEC coding rate, and digital symbol constellations).

In the rest of this work, since the focus is on the effect of channel modeling on the performance evaluation, rather than on finding the optimal AMC parameters and power margin balance, we consider the FEC coding rate and transmit spectral efficiency as given parameters, i.e., we consider a single e_i and set $\bar{e}_i = e_i$ in the transmit power expression (4). We focus then on the power margin setting, which, as described below, is a function of the wireless channel model.

Consider an interference-free link: in the presence of shadowing, flat or frequency selective fading, without adding a link margin (i.e.,

setting $M_{[\text{dB}]} = 0$ in 5), the achievable normalized information rate on a given subcarrier, given by $\log_2\left(1 + \xi_{i,q}^{(k)}\right)$, may drop below \bar{e}_i for a considerable percentage of the subcarriers (even with a null interference term in the denominator of (2)). The achievable amount of information in Eq. (3) is a random variable with a specific probability density function, which depends on the channel model in use. The link margin M is therefore set to guarantee a prescribed outage probability, i.e., that Eq. (3) is *not* satisfied with a probability lower than a given threshold, $p_{\text{tx,out}} \ll 1$. It is clear that the suitable M critically depends on the radio propagation aspects and frequency selectivity of the channels in a given deployment scenario and/or channel model. To take into account the link margin in our performance evaluation, we computed, through montecarlo simulations, the link margins required to guarantee an outage probability below 0,5%, assuming a FEC coding rate $K_{\text{ec}} = 0,8$, for the three channel models (out of the six channel models considered in this work, see Section 5.1) that present a stochastic component. As expected, the required link margins are different for the three stochastic channel models. The specific values are reported in the next section.

5. Performance evaluation

Before presenting our performance evaluation results, we preliminarily discuss, in the following subsection, the most relevant channel models features that may affect the performance evaluation accurateness. In Subsection 5.2 we describe the considered deployment scenarios, and in Subsection 5.3 we present our simulation results.

5.1. Channel models and implications

To describe the different models, let P_{tx} be the transmit power per subcarrier used by a transmitter, and $P_{\text{rx}}(d)$ the power received at a distance of d meters. In the following, all power values are expressed in mW or in dBm¹³. PL_{dB}

¹³In the latter case “dBm” appears as a subscript.

Table 1: Selected channel models

model	features
- M1 - Friirs Eq.	$PL_{[\text{dB}]} = 20 \log_{10} d_m - 27,56 + 20 \log_{10} f_{\text{MHz}}$
- M2 - Simple exponential decay model	$PL_{[\text{dB}]} = \begin{cases} 20 \log_{10} d_m - 27,56 + 20 \log_{10} f_{\text{MHz}} & d \leq d_0 \\ 10\eta \log_{10} d_m + K_{\text{dB}} + 20 \log_{10} f_{\text{MHz}} & d \geq d_0 \end{cases}$, $K_{\text{dB}} = (20 - 10\eta) \log_{10} d_0 - 27,56$. $\eta = 3, d_0 = 30 \text{ m}$
- M3 - METIS PL	Path loss only, with PL_{dB} given by Eq. 5-4, 5-5, 5-6 of [8]
- M4 - METIS PL+SH	Path loss plus Lognormal Shadowing (LSPs parameters from [8])
- M5 - METIS PL+SH+FD	Path loss + Lognormal Shadowing + Rice/Rayleigh flat fading, (LSPs parameters from [8])
- M6 - METIS PL+SH +FS	Path loss + Lognormal Shadowing + Rice/Rayleigh frequency selective fading, 13 paths per point-to point link (LSPs parameters from [8])

indicates the path loss in decibels ($PL_{\text{dB}} = P_{\text{tx,dBm}} - P_{\text{rx,dBm}}$). We consider the following six different channel models, enumerated as M1-M6. The considered models are also summarized in Table 1.

M1 is a simplistic channel model which accounts only for deterministic path loss as determined by the Friirs equation (see Table 1). This model assumes an exponential decay of received power as a function of distance, d , with an exponent $\eta = 2$, i.e., $P_{\text{rx}}(d) = K_F P_{\text{tx}}/d^2$, where K_F is a suitable constant.

M2 is a similar exponential decay model, with path loss exponent¹⁴ $\eta = 3$.

M3 PL is still a deterministic path loss model, which uses the path loss formulas 5-4, 5-5, and 5-6 of [8].

M4 - PL+SH, includes path loss and *spatially correlated* Lognormal shadowing, according to the parameters provided by [8].

¹⁴In order to be consistent with realistic power attenuation values, this model is typically considered valid for distances above a close-in reference distance d_0 . For distances below d_0 , a physical model like the Friirs equation is typically used. The selection of d_0 , besides that of the path loss exponent, has a *considerable* effect on the overall path loss.

M5 - PL+SH+FD, adds Rayleigh/Rician small scale fading (assumed to be flat across the frequency domain) on top of shadowing, with spatially correlated Rician K factors.

M6 - PL+SH+FS, includes frequency selective Rayleigh/Rician small scale fading. Using M6 entails the generation of the channel transfer function, evaluated at each subcarrier. The procedure to generate the transfer function taking in input the LSPs and other parameters, like number of scattering elements for each channel, delay spread proportionality factor, etc..., is provided in [8].

We assume omnidirectional antennas and radiation patterns, and Line Of Sight (LOS) conditions in each link. Therefore, Rician small scale fading is used for models M5 and M6. In this work, to parameterize the channel models, we consider the Urban Micro cell and Urban Macro cell scenario (UMi and UMa, respectively) of [9] for I2D communications, and the D2D channel parameters presented in [8] for D2D communications, see also Section 5.2.

The aim of our study is to evaluate how the performance of the offloading protocol depend on the channel model in use. To this end, before presenting our results, it is worth discussing the differences between the propagation loss entailed by the models M1-M3¹⁵, and the impact of the different statistics of the random components for models M4-M6. The following discussion provides useful insights for the interpretation of the results.

In Figure 1, we plot (in a dB scale) the propagation loss of the channel models M1-M3 as a function of distance. It can be seen that both the exponential decay models exhibit deviations from the more realistic propagation loss model M3 (which has been obtained in [8] through large scale measurements campaigns).

¹⁵The channel models M4-M6 are obtained by adding, to the propagation loss of M3, the shadowing (M4), flat fading (M5), and frequency selective fading (M6), random components. Therefore, Figure 1, and the related discussion, focus on M1-M3 only.

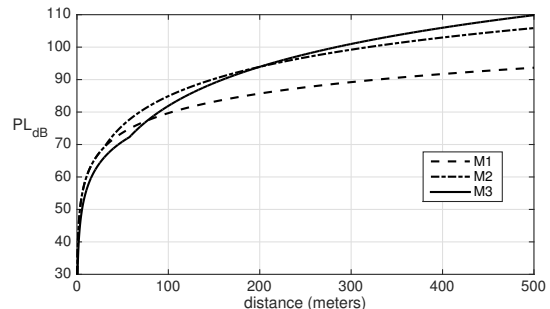


Figure 1: Deterministic path loss for models M1-M3.

Table 2: Selected link margin

Channel model	Channel scenario		
	V2V	UMi	UMa
M1-M3	5 dB	5 dB	4 dB
M4	5 dB	5 dB	4 dB
M5	12 dB	5 dB	13 dB
M6	13 dB	10 dB	11 dB

Particularly, M1 largely deviates for distances above 200 m, for which it underestimates the path loss term by more than 10 dB; M2 has the largest deviations (up to 10 dB), for distances in the range 10-150 m. These deviations may compromise the reliability of the results of the performance evaluation. In fact, both M1 and M2 entail an underestimation of the energy spent (on average) for I2D communications (which can reach distances well above 200 m), with respect to the energy spent for D2D communications (which are limited to distances in the order of 100 m). The main reason is that PL , under model M3, has a breakpoint distance (clearly visible in the figure, at a distance of 60 m), beyond which it increases (with distance) at a higher rate. Simple exponential decay models, regardless of the path loss exponent, are inherently smooth, and cannot reproduce the effect of the breakpoint distance.

Regarding the random components of the different models, namely Lognormal shadowing (introduced in M4), flat fading (introduced in M5) and frequency selective fading (introduced in M6), in Section 4.3 we have antic-

ipated that the different combinations of the random components, result in different statistics of the achievable amount of information. This affects the link margin selection, which is based on an outage constraint on the achievable amount of information, making it dependent on the assumed channel model. In our simulations, we have set the link margins on the basis of the results of preliminary montecarlo simulations aimed at determining, for each channel model, the link margin which guarantees an outage probability below 0,5 % assuming the presence of noise only. The results are summarized in Table 2¹⁶. During our system level simulations (described in the rest of this section), we have verified that the so selected link margins, thanks to the effectiveness of the RR scheduler in preventing strongly interfering links to use the same PRBs, are sufficient to guarantee a below 1% outage even in the presence of interfering links.

5.2. Deployment scenarios and traffic load settings

In our simulations, we have considered two deployment scenarios, hereafter denoted ad A and B, corresponding to a Urban micro-cell scenario and a Urban macro-cell one, as stadardized by the ITU (see e.g., [9]). In both deployment scenarios the ROI is a street chunk of length 3 Km and width 20 m. The two scenarios differ in the cell radius (and number of BSs) and in the antenna height of the BSs, as reported in Table 3.

Vehicles enter the street from both ends according to a Poisson arrival process with vehicle inter-arrival rate λ_V , and travel through it at

¹⁶For models M1-M3, it is not possible to compute the link margin based on an outage constraint, because the channel is deterministic, and hence there is no outage. The link margin, however needs to be present to guarantee the coexistence among interfering links. Therefore, in our simulations, we set, for model M1-M3, the same link margin used for model M4, which, as verified by us in the simulations, allows the RR scheduler to exploit spatial frequency reuse.

Table 3: Deployment scenarios parameters

Scenario	A	B
Number of BSs	6	4
BS positions (m)	0 m	0 m
	600 m	1000 m
	1200 m	2000 m
	1800 m	3000 m
	2400 m	
3000 m		
Cell diameter	600 m	1000 m
BSs antenna height	10 m	25 m
I2D channel model	Metis UMi*	Metis UMa**
D2D channel model	Metis V2V [†]	Metis V2V [†]
* Path loss: [8, Table 7-1] - UMi-O2O-(BS-UE)-LOS Random components LSPs: [8, Table 7-2] - UMi-LOS		
** Path loss: [8, Table 7-1] - UMa-O2O-(BS-UE)-LOS Random components LSPs: [8, Table 7-2] - UMa-LOS		
† Path loss: [8, Table 7-1] - UMi-O2O-D2D/V2V Random components LSPs: [8, Table 7-3] - D2D&V2V-O2O-LOS		

constant speed. The speed of each vehicle is randomly selected from a uniform distribution in the range $[v_a, v_b]$ m/s and is kept constant during the whole path. We have performed simulations for three different speed range settings, namely [6,16], [9,24], and [12,32] m/s.

The content requests arrival process of each device is modeled as a Poisson arrival process with inter-arrival rate λ_C , and the content popularity is modeled by a Zipf distribution with parameter α , i.e., numbering the available contents as $k = 1, 2, \dots$, the probability that a device requests content k is $p(k) = \frac{1}{\zeta(\alpha)} k^{-\alpha}$, where $\zeta(\cdot)$ is the Riemann ζ -function.

We set the following parameters which determine the traffic load: $\lambda_V = 20$ new vehicles per minutes, each vehicles generates content requests with an average rate $\lambda_C = 6$ requests per minute, and the content payload size is $L = 432$ kB.

We measure the average offered traffic load in terms of a traffic load spatial density ρ_Q . Since our scenario is (essentially) unidimensional, we consider a linear density (instead of a surface density), and express ρ_Q in kbps/m. Hence, ρ_Q represents the average number of bits requested by the devices located in a street chunk of length 1 m (and width equal to the street width). ρ_Q is the product of the average number of vehicles present in a street chunk of

length 1 m, say ρ_V ¹⁷, times the content request arrival rate per user λ_C , times the coded packet size D , times the ratio, which we indicated with γ_{nr} , of non-repeated request to total requests¹⁸, i.e., $\rho_Q = \lambda_C \rho_V D \gamma_{nr}$ kbps/m. For the three considered vehicles speed ranges [6,16], [9,24], and [12,32] m/s, we obtain $\rho_Q = 13.9, 9.26,$ and 6.95 kbps/m, respectively.

A conventional cellular system with BSs deployed on a straight line, a spatial frequency reuse factor of 1/3, and cell diameter d_c , can support a maximum traffic load density equal to $\rho_{Q,max}^{(I2D)} = W e / 3 / d_c = 36$ kbps/m, considering the cell diameter of Scenario A, and 21 kbps/m, considering scenario B.

All the system parameters are summarized in Table 4.

5.3. Simulation results

For each deployments scenario (A,B), each traffic model input, and each channel model M1-M6, we run 10 simulations using i.i.d. random realizations of the vehicles arrival process, the content requests process, and (for channel models M4-M6 only, since M1-M3 are deterministic models) the spatially correlated random channels set. For each realization of the random temporal and spatial processes, we run a system simulation of 30 minutes¹⁹.

Figure 2 displays the offloading efficiency (with 95% confidence intervals), defined as

¹⁷For a uniform distribution of the speed range in an interval $[v_a, v_b]$ m/s, the average linear density of the vehicles is given by $\rho_V = \lambda_V (\ln(v_a^{-1}) - \ln(v_b^{-1}) / (v_b - v_a))$ [13].

¹⁸Since the content requests are assumed to be i.i.d, there is a non negligible probability that a device makes the request of a content it already has in its cache. Repeated requests are simply discarded by the CDMS, whereas the sharing timeout counter is reset to its starting value τ_s . In [13, Lemma 4], we computed the ratio of non-repeated to total requests, here indicated with γ_{nr} . For the specific settings considered here, for content request processes, we obtain $\gamma_{nr} \simeq 0.59$.

¹⁹To enable a fair comparison among the channel models, we used, for each channel model, the same 10 i.i.d. realizations of the vehicles arrival and content request processes.

Table 4: System parameters used for performance evaluation

System parameter	symbol	value
Speed range	$[v_a, v_b]$	[3, 8], [9, 24], [12, 32] (m/s)
Vehicles arrival rate (new vehicles per minute)	λ_V	20
Average number of vehicles in the ROI	-	98, 65, 49
Content requests per minute (for each vehicle)	λ_C	6
Content payload size	L	432 kB
Coded packet size	D	540 kB
Zipf distribution parameter for the content popularity	α	1,1
Content timeout	τ_c	20 s
Sharing timeout	τ_s	600 s
Center frequency of the system band	f_0	2.3 GHz
System bandwidth	W	10.8 MHz
CI Duration	T_{CI}	1 s
PRB duration	τ	0.5 ms
PRB bandwidth	w	180 KHz
Number of subcarriers per PRB	n_c	12
Subcarrier spacing	w_c	15 KHz
Noise power spectral density	N_0	-174 dBm
Receiver noise figure	F	10 dB
Link margin	M	See Table 2
Forward error correction coding rate	K_{ec}	4/5
Normalized transmission rate	e_i	6

the percentage of contents delivered through offloading, i.e., using D2D communications, achieved under scenarios A (Figure 2.a) and B (Figure 2.b). Each bar color refers to a different speed range setting. In general, with the considered vehicles traffic parameters, an offloading efficiency around 40% is achieved. It can be seen that, with higher speed ranges, there is a decrease of the offloading efficiency due to the decreasing vehicles density. The decrease of offloading efficiency, however, is quite small. This is the effect of delay-tolerance: with higher speed ranges, the number of vehicles encountered by each device during the content timeout of each request increases, thus counterbalancing the decreased vehicles density. In the absence of delay tolerance, the decrease in offloading efficiency would be much higher. Offloading efficiency is not affected either by the deployment scenario, or the channel model. This is

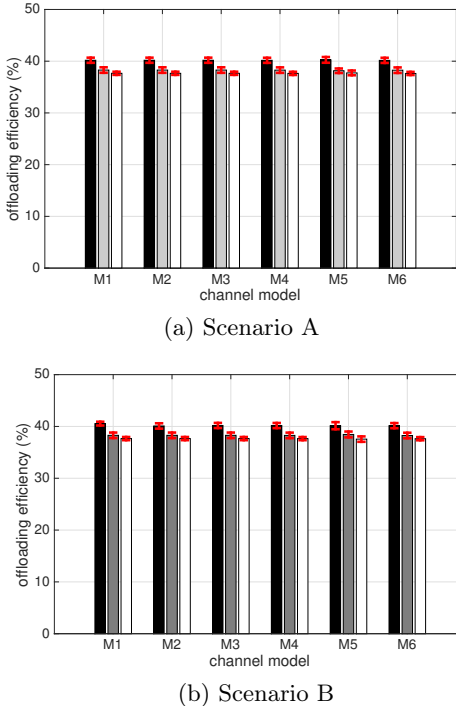


Figure 2: Offloading efficiency in deployment scenario A and B, for speed range [6,16] (black bars), [9,24] (grey bars), [12,32] (white bars).

due to the fact that the CDMS schedules D2D offloading as a function of nominal channel gain rankings, which depend only on distance.

Figure 3 displays the average energy consumption (with 95% confidence intervals over the set of simulations) of the entire system (i.e., including the energy spent by both I2D and D2D content deliveries) measured in mJ per delivered content, obtained in Scenario A. Figure 3.a refers to the benchmark I2D-only scheme, and Figure 3.b to the CDMS-aided D2D data offloading scheme.

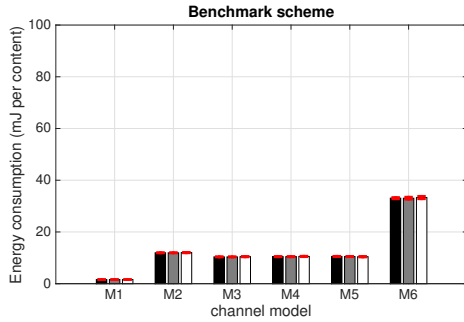
Figure 4 refers to the same performance metric, obtained under Scenario B. It can be seen that there is a considerable mismatch among the performance obtained using different channel models. Notably, the flat fading model M5, in the case of Scenario B, tends to overestimate the energy consumption, with respect to the frequency selective model M6, whereas in Scenario A it is the opposite. This is due to the

fact that the required power link margin for I2D communications, computed using M5, is higher than the one computed using M6 under Scenario B, and lower under Scenario A (see Table 2). The link margin, computed on the basis of an outage constraint, captures specific differences in the statistics of the frequency selective channels behavior macro-cells and micro-cells. In general, higher antenna heights (25 m under Scenario B, opposed to 10 m under Scenario A) entail a lighter tail of probability density function of the achievable amount of information, which turns out in lower required link margin to satisfy the outage constraint. This realistic behavior, however, is not well captured by the flat fading channel model M5, thus leading to the mismatch.

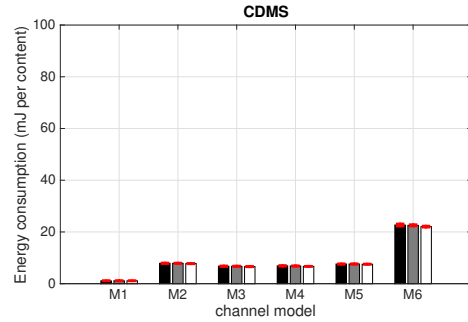
Figure 5 shows the estimation of the energy savings percentage of the CDMS-aided D2D offloading scheme with respect to the benchmark scheme under Scenario A (Figure 5.a) and Scenario B (Figure 5.b). With Scenario B, the estimation seems to be consistent for all the channel models (with deviation below 2%). Under Scenario A, however, mismatches in the order of 4% energy saving can be observed, with the worst performing model M5 entailing a 6% underestimation of the achievable energy saving gain.

Figures 6 and 7 report the percentage of the spectrum usage for scenarios A and B, respectively. In each CI, each PRB is counted as being used if it is allocated to at least one communication over the entire ROI. The effect of spatial frequency reuse is visible since the CDMS-aided offloading scheme (Figures 6.b and 7.b) uses less PRBs than the benchmark scheme (Figures 6.a and 7.a). In this case, the deterministic channel models M1 and M2 provide unreliable results, overestimating spectrum occupation when considering the CDMS-aided scheme, whereas the results obtained with models M3-M6 are consistent.

The same problem with M1 and M2 arises when considering the relative gain in spectrum

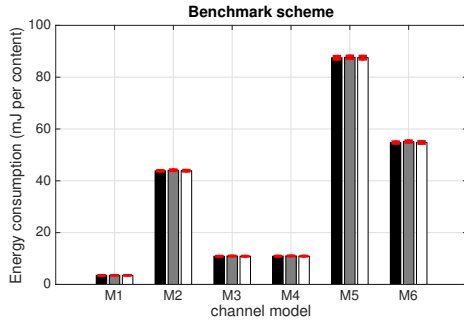


(a) Benchmark I2D-only scheme

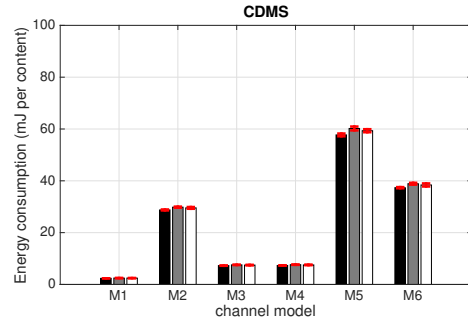


(b) CDMS-aided offloading scheme

Figure 3: Energy consumption for the benchmark and CDMS-aided offloading schemes in Deployment Scenario A. Speed range [6,16] (black bars), [9,24] (grey bars), [12,32] (white bars).



(a) Benchmark I2D-only scheme



(b) CDMS-aided offloading scheme

Figure 4: Energy consumption for the benchmark and CDMS-aided offloading schemes in Deployment Scenario B. Speed range [6,16] (black bars), [9,24] (grey bars), [12,32] (white bars).

occupation, displayed in Figure 8. In this case, the mismatch is considerable.

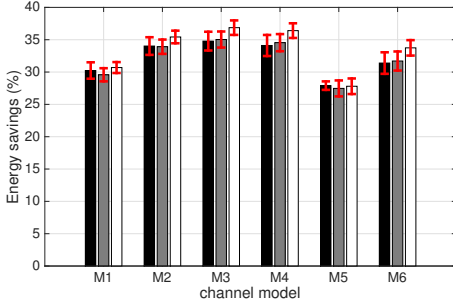
The use of the deterministic models M1 and M2 (with the considered link margin settings) tend to underestimate the possibility to spatially reuse the spectrum, as the percentage spectrum occupation reduction ranges (depending on the scenario, A or B, and the channel model, M1 or M2) from 5% to 21%, while, when using channel models M3-M6, it is between 31% and 35% for the different speed ranges.

The gain estimated with the simplistic models, in this case, is completely unreliable. For instance, it can be up to six times less (with M1) than the what is estimated by the more

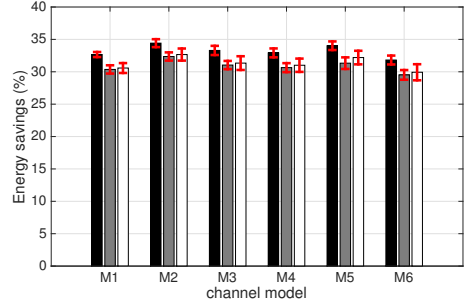
accurate channel models. This happens due to the effect explained in Figure 1, i.e., the underestimation of the channel gain difference between short ranges and long ranges, for both models M1 and M2. This underestimation turns into an overestimation of the interference among potentially concurrent D2D links. As the RR scheduler takes the estimated interference as an input, it tends to separate potentially concurrent links more than actually necessary.

6. Conclusion

In this work, we have studied the performance of a D2D-based traffic offloading protocol for highly dynamic scenarios like vehicular environments. We have evaluated its performance in terms of energy efficiency and system

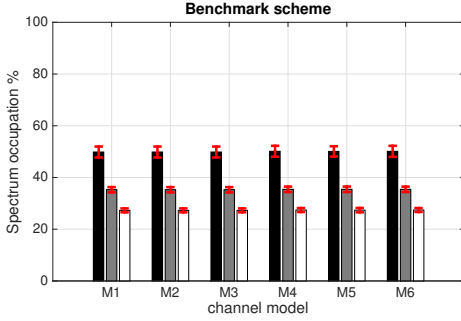


(a) Scenario A

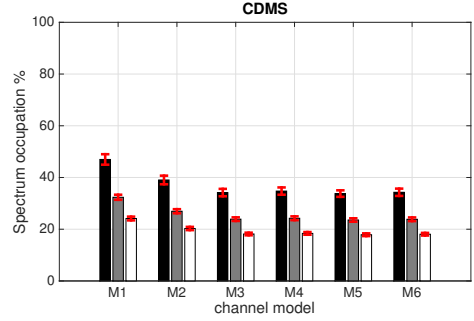


(b) Scenario B

Figure 5: Energy savings percentage in Scenarios A and B; speed range [6,16] (black bars), [9,24] (grey bars), [12,32] (white bars).



(a) Benchmark I2D-only scheme

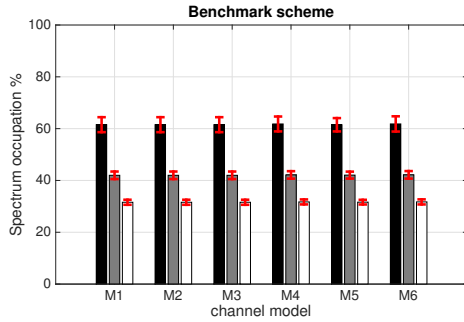


(b) CDMS-aided offloading scheme

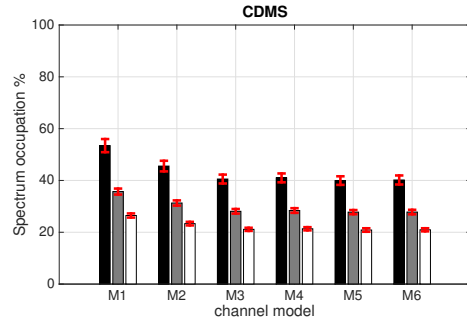
Figure 6: Spectrum occupation percentage obtained with deployment scenario A for the benchmark and the CDMS-aided schemes; speed range [6,16] (black bars), [9,24] (grey bars), [12,32] (white bars).

spectral efficiency, by considering a selection of different, increasingly detailed, wireless channel models. We have showed that the considered protocol can achieve substantial improvements in terms of power consumption and system-wise spectral efficiency (compared to a scheme that only uses I2D communications). Specifically, for the vehicles traffic parameter settings used in our study, we have observed a 35% energy consumption reduction gain and a 35% reduction of spectrum use, with respect to a benchmark scheme which uses classical I2D communications only. In terms of spectral *efficiency* (measured in bps/Hz), a 35% reduction of spectrum use corresponds to a 50% increase.

Taking the channel model M6 (the most realistic channel model among those considered in this work) as a reference, we have shown that the simpler channel models, because they do not capture many aspects of the radio propagation, are not able to consistently and reliably evaluate the performance metrics. More specifically, we have seen that the use of any of the models M1-M5, is either considerably unreliable or, in the cases it provides an estimation of one of the considered performance metrics (energy consumption and spectral occupancy) close to the one provided by model M6, it fails to do so with the other one. We have provided insights on the reasons of this behavior, pointing out the major weaknesses of the considered channel models: the mismatch of simple propagation loss formulas (in M1, M2) with respect

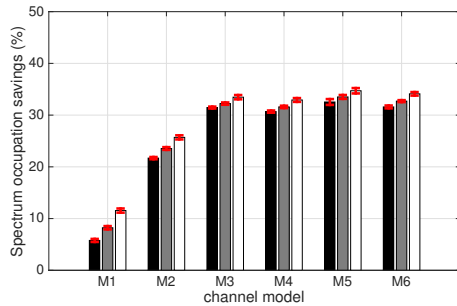


(a) Benchmark I2D-only scheme

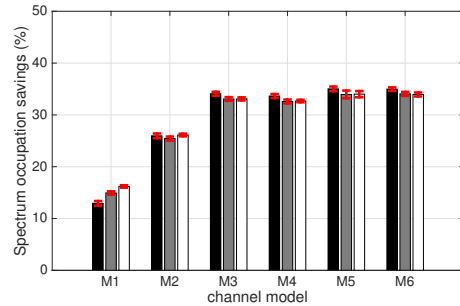


(b) CDMS-aided offloading scheme

Figure 7: Spectrum occupation percentage obtained with deployment scenario B for the benchmark and the CDMS-aided schemes; speed range [6,16] (black bars), [9,24] (grey bars), [12,32] (white bars).



(a) Scenario A



(b) Scenario B

Figure 8: Spectrum occupation savings: relative percentage of non-used spectrum for with the CDMS-aided scheme, with respect to the amount of spectrum used by the benchmark scheme; speed range [6,16] (black bars), [9,24] (grey bars), [12,32] (white bars).

to formulas obtained through large measurements campaigns; the absence, in M1-M3, of random fluctuations around the mean path loss due to shadowing and small scale fading; and the lack of representation of the frequency selectivity (in M1-M5). The overlooking of either of these aspects prevents to correctly take into account important system parameters, like the link margin and the FEC coding gain, which are quite important for a system-level design and performance evaluation. Our analysis and discussion, suggest that the performance evaluation of offloading schemes based on a channel model, like M6, that captures the effects of real-life propagation losses and channel frequency selectivity. The use of accurate channel models, paired with a suitable physical layer model, provides much more insights on the effects of

physical layer parameters with respect to the popular approach of using simplistic models, and should play a significant role in the design of offloading schemes, further optimized taking into account the above described effects.

Acknowledgement

This work was partially funded by the EC under the H2020 REPLICATE (691735), So-BigData (654024) and AUTOWARE (723909) projects.

References

- [1] F. Rebecchi et al., Data Offloading Techniques in Cellular Networks: A Survey, *IEEE Communications Surveys & Tutorials* 17 (2) (2015) 580–603.
- [2] R. Bruno, A. Masaracchia, A. Passarella, Offloading through opportunistic networks with dynamic content requests, in: *Proc. 15th IEEE International Conference on Mobile Ad-hoc and Sensor*

- Systems (MASS '14), Philadelphia, PA, USA, Oct. 27-30, 2014.
- [3] J. Whitbeck, Y. Lopez, J. Leguay, V. Conan, M. D. de Amorim, Push-and-track: Saving infrastructure bandwidth through opportunistic forwarding, in: Pervasive and Mobile Computing, Vol. 8, 2012, pp. 682–697.
 - [4] M. V. Barbera, A. C. Viana, M. D. De Amorim, J. Stefa, Data offloading in social mobile networks through VIP delegation, Elsevier Ad Hoc Networks 19 (2014) 92–110.
 - [5] F. Rebecchi, L. Valerio, R. Bruno, V. Conan, M. D. De Amorim, A. Passarella, A joint multicast/D2D learning-based approach to LTE traffic offloading, Computer Communications 72 (2015) 26–37.
 - [6] F. Rebecchi, M. Dias de Amorim, V. Conan, Circumventing plateaux in cellular data offloading using adaptive content reinjection, Computer Networks 106 (2016) 49–63.
 - [7] IST WINNER II Project Deliverable 1.1.2, WINNER II Channel Models, Part I, Tech. rep. (2007).
 - [8] ICT METIS Project Deliverable 1.4, METIS Channel Models, Tech. rep. (2015).
 - [9] ITU-R M.2135-1, Guidelines for evaluation of radio interface technologies for IMT-Advanced, Report M.2135-1, International Telecommunication Union (ITU) (Dec. 2009).
 - [10] 3GPP, Study on 3D channel model for LTE (Release 12), T.R. 36.873, V12.4.0, 3rd Generation Partnership Project; Technical Specification Group Radio Access Network (03 2017).
 - [11] Y. Yang, T. Liu, X. Ma, H. Jiang, J. Liu, FRESH: Push the Limit of D2D Communication Underlying Cellular Networks, IEEE Tran. Mob. Comput. 16 (6) (2017) 1630–1643.
 - [12] L. Pescosolido, M. Conti, A. Passarella, Performance evaluation of an energy efficient traffic offloading protocol for vehicular networks, in: Proc. 1st International Balkan Conference on Communications and Networking (BalkanCom '17), Tirana, AL, May 30-Jun 2, 2017.
 - [13] L. Pescosolido, M. Conti, A. Passarella, Performance analysis of a device-to-device offloading scheme for vehicular networks, in: Proc. 19th IEEE International Symposium on a World of Wireless, Mobile and Multimedia Networks (WoWMoM '18), Chania, Greece, Jun. 12-15, 2018.
 - [14] Y. Shi, Y. T. Hou, J. Liu, S. Kompella, How to correctly use the protocol interference model for multi-hop wireless networks, Proc. 10-th ACM international symposium on Mobile ad hoc networking and computing (MobiHoc '09), New Orleans, LA, USA, May 18 - 21, 2009.

Appendix: Radio resource allocation for coexisting I2D and D2D links

The “full resource sharing” approach [11] builds on the idea of *radio resource set partitioning*. Conceptually, the procedure requires two stages: first, the overall set of links to be scheduled (both I2D and D2D links) is partitioned into subsets, called resource reuse sets; second, each resource reuse set of links is assigned a subset of the radio resources (the PRBs) available in a CI. In [11], both stages are performed in one-shot, having in input the transmit power of each link²⁰. The second stage also includes the possibility to prune some resource reuse sets from the scheduling of the set of resources in order to guarantee I2D communications (which have an higher priority).

Our RR scheduler is inspired by the scheduler proposed in [11] but differs from it in several aspects. Specifically, our implementation copes with the more realistic assumptions of multiple cells, independent power setting for each transmission, and frequency selective channels. Furthermore, it guarantees that if a link is admitted to be scheduled in a given CI, it will receive an amount of resources sufficient for transmitting the whole desired content.

The whole scheduling procedure is sketched out in the diagram in Figure 9. Here, for space reasons, we omit the details of the procedure, and just highlight the most important features.

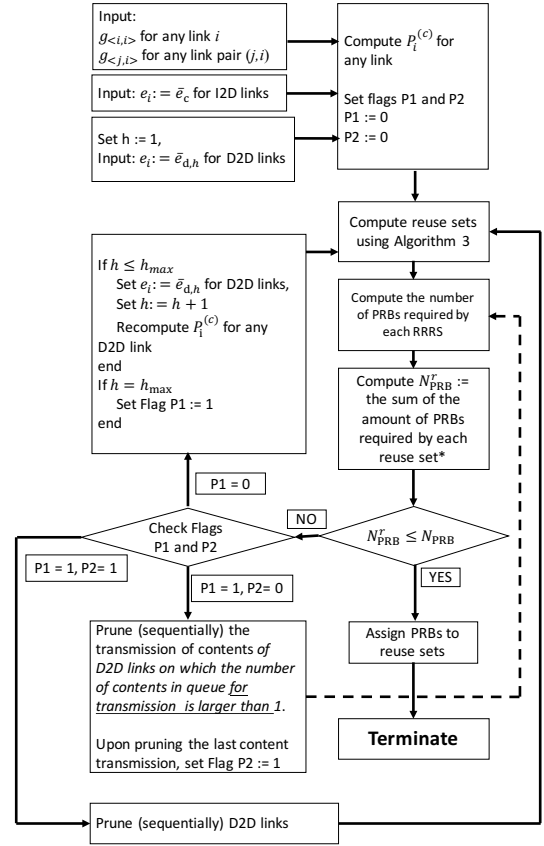
Rather than working at the link level only, we deal with the individual I2D and D2D packet transmissions that the CDMS has established as candidates for being scheduled. A single link may be required to transmit one, *or more*, packets during a CI. The scheduler inputs are: all the nominal channel gains between any link pair $\langle j, i \rangle$; for I2D links, a prescribed value of the target normalized nominal information rate $e_i = \bar{e}_c$, equal for all the I2D

²⁰In [11], the transmit power is assumed to have a common value for all I2D links, and another common value for all D2D links.

links; for D2D links, a set of candidate values for the target normalized nominal information rate $\bar{\mathcal{E}}_d = \{\bar{e}_{d,1}, \dots, \bar{e}_{d,h_{\max}}\}$. The computation of the per-subcarrier power levels, performed by the scheduler, follows from Eq. (5).

Now, if the modulation scheme in use has a maximum transmit spectral efficiency, say e bps/Hz, it makes no sense that the target normalized information rate is set with a value larger than e , since the physical transmission system will be in any case not able to transmit bits with such a rate. Therefore, we set \bar{e}_c to be the maximum allowed spectral efficiency among the modulation formats in use, and $\bar{\mathcal{E}}_d$ to be the set of values for the transmit spectral efficiencies entailed, for example, by a set of possible constellations that the D2D links can use. The rationale behind this choice is as follows: first, for I2D links, which by definition cannot share resources among them, the ideal thing to do is to use as few PRBs as possible, in such a way to leave more room for the other I2D communications. This is achieved by using the maximum transmit spectral efficiency. However, to actually manage to communicate the desired amount of information, a suitable power is required on each subcarrier, and this power is determined by Eq. (5). Second, for D2D links, which can share resources with other D2D links (and with I2D links), since the resource reuse subsets will tend to favor the coexistence of links with low cross-interference, the ideal thing to do is to maximize the number of used resources, in such a way to minimize the overall transmit power used to transmit a content²¹. For this reasons, the value of e_i for D2D links, in the resource allocation procedure, is initialized with the lowest value in $\bar{\mathcal{E}}_d$, and the corresponding required power to support that rate is computed according to Eq. (5). During the procedure, after the computation of the radio resource reuse sets

²¹In general, in a radio communication, the larger the available bandwidth, the lower the power required to obtain a desired capacity.



* This computation takes into account the resource sharing of PRBs among the links.

Figure 9: Diagram of the considered radio resource allocation procedure.

(see below) and of the number of total required PRBs, N_{PRB}^r , it may happen that the currently selected value of e_i for D2D links prevents to accommodate all the required transmissions, i.e., it results in $N_{\text{PRB}}^r > N_{\text{PRB}}$. In this case, the scheduler iteratively increases the desired target nominal normalized information rate e_i for D2D links, it recomputes the resource reuse sets and the corresponding number of total required PRBs, and it re-checks if $N_{\text{PRB}}^r > N_{\text{PRB}}$. If no value of e_i for D2D links, compatible with the requirement $N_{\text{PRB}}^r \leq N_{\text{PRB}}$, is found, the procedure starts to exclude D2D packets from those admitted for transmission in the current CI, and then entire D2D links, until a subset of admissible D2D links and D2D packets (each link can transmit one or more packets) to be transmitted, compatible with the requirement $N_{\text{PRB}}^r \leq N_{\text{PRB}}$, is found.

The details of the computation of the resource reuse sets are summarized by Algorithm 3, which is based on [11, Algorithm 1]. The following notation is required to interpret Algorithm 3: let S^c and S^d be the sets of I2D and D2D links among which the radio resources need to be partitioned, with $S = S^c \cup S^d$. Let S_r^c and S_r^d be the set of cellular and D2D links in the r -th radio resource reuse set $S_r = S_r^c \cup S_r^d$ in the partition $S = \uplus_r S_r$, which is the output of Algorithm 3. We indicate with $b(i)$ the base station to which the receiver of the I2D link i is associated and with $\{S_1^c, \dots, S_{N_{BS}}^c\}$ a partition of the link set S^c , where $i \in S_b^c$ iff $b(i) = b'$, or $S_b^c = \{i \in S^c \mid b(i) = b'\}$. Finally, we indicate with $\hat{P}_r(b, i) = \operatorname{argmax}_{j \in S_b^c} (P_j^{(c)} g_{(j,i)})$ the maximum (nominal) interference that a D2D link i can receive, on a single subcarrier, from a I2D link which is in the same resource reuse set as link i , and is handled by BS b . Finally, let CL represent a running set of candidate links, initialized with the whole set S of links to be scheduled.

Algorithm 3 results from [11, Algorithm 1] replacing the minimum SNIR constraints [11, Equations (2a) and (2b)] with

$$\log_2 \left(1 + \frac{P_i^{(c)} g_{(i,i)}}{\sigma_c^2 + \sum_{j \in S_r^d} P_j^{(c)} g_{(j,i)}} \right) \geq e_i, \quad \forall i \in S_r^c, \quad (6)$$

$$\log_2 \left(1 + \frac{P_i^{(c)} g_{(i,i)}}{\sigma_c^2 + \sum_{b \in \mathcal{B}} \hat{P}_r(b, i) + \sum_{j \in S_r^d \setminus \{i\}} P_j^{(c)} g_{(j,i)}} \right) \geq e_i, \quad \forall i \in S_r^d,$$

and the Resource Sharing Conditions (RSC) in [11, Equations (9) and (17)], with RSC-1:

$$\sum_{j \in S^d \setminus \{i\}} P_j^{(c)} g_{(j,i)} < \frac{P_i^{(c)} g_{(i,i)}}{(1 + |S^d| \xi_h) |S^d| - 1} - \sigma_c^2, \quad \forall i \in S^d, \quad (7)$$

$$\text{where } \xi_h = \max_{i \in S^d} \frac{P_i^{(c)} g_{(i,i)}}{w N_0},$$

Algorithm 3 Radio Resource Set Partitioning

```

1:  $r = 1$ 
2: while  $CL \neq \emptyset$  do
3:    $S_r = CL$ 
4:   // Trim  $S_k$  according to the set of inequalities (6)
5:   compute  $\check{e}_i \forall i \in S_r$ ;
6:   find link  $i^* \in S_r$  with minimum  $\check{e}_i$ ;
7:   while  $\check{e}_{i^*} < e_i$  do
8:     remove  $i$  from  $S_r$ ;
9:     compute  $\check{e}_i \forall i \in S_r$ 
10:    find link  $i^* \in S_r$  with minimum  $\check{e}_i$ ;
11:  end while
12:  // Trim  $S_r$  according to RSC1 and RSC2,
13:  find  $S^* \subset S_r$  of the links not satisfying the sets of
  inequalities (7) and (8);
14:  while  $S^* \neq \emptyset$  do
15:    compute  $\check{e}_i \forall i \in S^*$ ;
16:    find link  $i^* \in S^*$  with minimum  $\check{e}_i$ ;
17:    remove  $i^*$  from  $S_r$ ;
18:    find  $S^* \subset S_r$  of links not satisfying the inequalities
  (7) and (8);
19:  end while
20:  remove link members of  $S_r$  from  $CL$  and set  $k = k + 1$ ;
21: end while

```

and RSC-2:

$$\begin{cases} \sum_{j \in S^d} P_j^{(c)} g_{(j,i)} \leq \frac{P_i^{(c)} g_{(i,i)}}{(1 + |S^d| \xi_h) |S^c| + |S^d| - 1} - \sigma_c^2, \quad \forall i \in S^c \\ \sum_{j \in S^c \setminus \{i\}} P_j^{(c)} g_{(j,i)} \leq \frac{P_i^{(c)} g_{(i,i)}}{(1 + |S^d| \xi_h) |S^c| + |S^d| - 1} - \sigma_c^2, \quad \forall i \in S^d \end{cases}, \quad (8)$$

$$\text{where } \xi_h = \max \left(\max_{i \in S^d} \frac{P_i^{(w)} g_{(i,i)}}{\sigma_c^2}, \max_{i \in S^c} \frac{P_i^{(w)} g_{(i,i)}}{|S^d| \sigma_c^2} \right)$$

respectively.

Finally, in Algorithm 3, the term \check{e}_i represents a lower bound on the nominal normalized information rate achievable of link i , and is defined as

$$\check{e}_i = \begin{cases} \log_2 \left(1 + \frac{P_i^{(c)} g_{(i,i)}}{\sigma_c^2 + \sum_{j \in S_r^d} P_j^{(c)} g_{(j,i)}} \right), & \forall i \in S_r^c, \\ \log_2 \left(1 + \frac{P_i^{(c)} g_{(i,i)}}{\sigma_c^2 + \sum_{b \in \mathcal{B}} \hat{P}_r(b, i) + \sum_{j \in S_r^d \setminus \{i\}} P_j^{(c)} g_{(j,i)}} \right), & \forall i \in S_r^d. \end{cases}$$